**NUEJ**
**Naresuan University**
**Engineering Journal**

# Demagnetization Fault Detection on BLDC by Adaptive Neuro Fuzzy Inference System

Kreangsuk Kraikitrat[1,] and Bunyarit Wangngon[2*]

[1] Department of Electrical Engineering, Faculty of Engineering, University of Phayao, Phayao, Thailand
[2] Department of Electrical Engineering, Faculty of Engineering Rajamangala University of Technology Lanna Phitsanulok, Thailand

* Corresponding author e-mail: maxaee_@hotmail.com

(Received: 30 September 2021, Revised: 20 October 2021, Accepted: 2 November 2021)

**Abstract**

This research presents a method for detecting permanent magnet damage anomalies in a brushless direct current motor (BLDC Motor) by applying the adaptive neuro-fuzzy interface system (ANFIS). The input data for ANFIS has 4 lead inputs. Derived from the magtitude and position of the third order harmonics of the stator current and back electromotive force (Back-EMF) from the BLDC Motor. Consists of frequency of 3rd Order in the Back-EMF, magnitude of 3rd Order in the Back-EMF, frequency of 3rd Order in the Motor Current and Magnitude of 3rd Order in the Motor Current. The ANFIS construction is ideal for detecting any malfunctions. It is the combined structure of the fuzzy logic system (FLS) and artificial neural networks (ANN) methods. In the FLS part, the membership function is used as the triangular and choose the principle of function approximation as sugeno fuzzy model and in ANN choose feed-forward network, there is transfer function at hidden layer and output layer is tan-sigmoid transfer function (tansig) and linear transfer function (purelin) respectively and have a learning style back-propagation learning from the test, it was found that the learning error of ANFIS was 3.62E-03 and the accuracy in the detection of anomalies was 98.81%.

**Keywords:** Brushless Direct Current Motor, Demagnetization, Back Electromotive Force, Stator Current, Adaptive Neuro-Fuzzy Interface System.

## 1. INTRODUCTION

Nowadays, Brushless Direct Current Motor (BLDC Motor) is widely used in various industrial sectors, especially in the electric vehicle and electric bicycle industry. Due to its good power transmission properties carbon brushes are not required to transmit power like a brushed direct current motor (DC Motor). BLDC Motor is a type of machine that has malfunctions. The cause may be caused by the motor manufacturing process or caused by abnormal operating conditions. Faults that occur can occur in many parts such as bearing faults, stator faults and demagnetization faults etc. Faults in a BLDC Motor are divided into 2 The main categories include electrical faults and mechanical faults. Research (Albrecht et al., 1986) has shown that the percentage of motor faults occurring is found to be the majority of bearing damage. used followed by faults occurring at the stator and rotor in order.

There are two methods of checking motor faults at present, checking by stopping the motor. For example, checking the fracture of the permanent magnet, the deterioration of the bearing, which this method has a disadvantage is that it has to stop the work process. Due to such disadvantages, there is another way to check without stopping the motor is an analysis of abnormalities caused by electrical signals such as voltage, current, etc., which helps to identify impending motor faults before they can cause serious damage. In research (Kang et al., 2015; Kang et al., 2015; Yang et al., 2021; Usman & Rajpurohit, 2020; Usman et al., 2020; Usman et al., 2019; Kim & Hur, 2016; Kim et al., 2020; Kim et al., 2010; Usman & Rajpurohit, 2020; Madhav & Sadakale, 2020; Kim et al., 2020) The study and analysis of back electromotive force (Back-EMF). From the damage condition incurred to the permanent magnet in the BLDC Motor by analyzing the electrical signal. Voltage and other parameters.

In the study (Mati & Kuli, 2010; Drira & Derbel, 2011; Kolla & Altman, 2007) applied artificial neural networks (ANN) to detect and classify abnormalities in rotor and stator of the motor by taking electrical signal data. The resulting vibration and heat are inputs for ANN to be used in the learning process and analyze the network output for discriminative analysis of motor faults.

In the study (Dias & Chabu, 2008; Zouzou et al., 2009; Laala et al., 2011) applied fuzzy logic system (FLS) to detect and classify abnormalities in rotor and stator of the motor by taking the information of the electric signal, vibration and heat generated. Define and create. Membership function in the FLS method for discriminating motor faults.

Different mathematical methods have their advantages and disadvantages, and no one is better than the other in every way. An ANN, for example, has the advantage of being able to learn and recognize patterns. But there is a disadvantage that it cannot explain the reason for the

decision while FLS. It is characterized by its logical reasoning like human thought. Decisions can be explained by FLS rules and can be applied to obscure information. But the disadvantage of FLS lies in the inability to learn and customize the rules by yourself. Must rely on experts or knowledgeable people to define the structure and rules. Therefore, researchers are interested in combining different methods into a hybrid system in order to combine the advantages of each method and eliminate the limitations of each method. One such hybrid system is the ANN blending with FLS to form the Adaptive Neuro-Fuzzy Interface System (ANFIS) proposed by J.S.r. Jang (Kolla & Altman, 2007)

In the study (Souad et al., 2017; Moghadasian et al., 2017; Ballal et al., 2007) the application of ANFIS to the analysis of motor abnormalities was presented. which is a system created by the combined application of FLS or fuzzy logic with ANN In order to distinguish between motor faults.

This research applied ANFIS to detect abnormality caused by permanent magnet damage in BLDC Motor rotor. The input data for ANFIS has 4 inputs taken from Third order harmonics (3rd order):

1. Frequency of 3rd Order in the Back-EMF
2. Magnitude of 3rd Order in the Back-EMF
3. Frequency of 3rd Order in the Motor Current
4. Magnitude of 3rd Order in the Motor Current

The working process of rotor permanent magnet detection and classification system by applying ANFIS started simulating the state of permanent magnet fracture in BLDC motor into 3 case studies as follows: 1. Normal permanent magnet (0BB) 2. Permanent magnet damaged 1 bar conductor (1 BB) and 3. Two permanent magnets damaged (2BB). Stator current and back-EMF signals with the motor operating under various simulation conditions are analyzed and converted from time domain to frequency domain signal (Fast Fourier Transform (FFT)) to continue as input in ANFIS.

## 2. BRUSHLESS DIRECT CURRENT MOTOR

### *2.1 Fundamental of BLDC motor (Kim et al., 2020)*

A BLDC motor is usually supplied with a 120-degree commutation inverter and the schematic of a BLDC motor drive circuit is shown in Fig. 1.

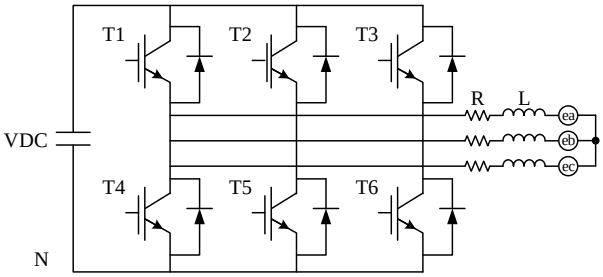


**Figure 1** Schematic of a BLDC motor drive circuit.

In this paper, an upper PWM method for a speed controller is used. An illustration of the ideal back-EMF, current waveform and the switching states in a BLDC motor is shown in Fig. 2.

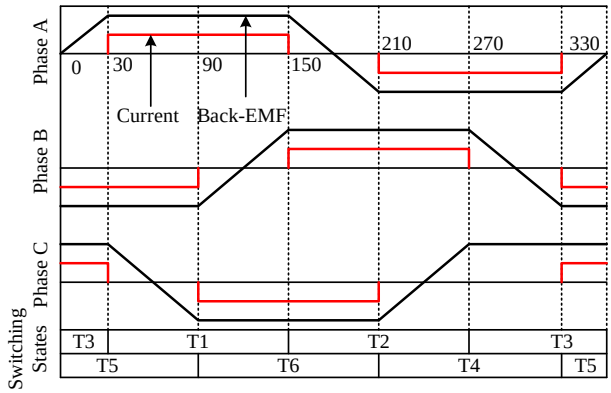


**Figure** 2 The ideal waveforms of back-EMF, current and witching states.

### *2.2 Demagnetization faults in BLDC motor (Usman & Rajpurohit, 2020)*

Additional investigations are made on the harmonic analysis of demagnetization faults in the BLDC motor drive. The harmonics are excited at multiples of mechanical frequency in the stator back-EMF and current spectrum as given in (1).

$$f_{demag} = f_s\left(\frac{k}{p/2}\right) = kf_m \qquad k = 1,2,3... \qquad (1)$$

where $f_{demag}$ is the frequency of $k^{th}$ component in the spectrum, $f_s$ is electrical frequency, $f_m$ is the rotational frequency and $p$ is the number of poles. The proposed investigations are done on the BLDC motor under study with $p$ = 12.

### *2.3 BLDC motor Operation (Faiz & Mazaheri, 2017)*

In this section, the effect of the demagnetization fault on Back-EMF waveforms of a BLDC motor is studied; harmonics of Back-EMF, caused by the demagnetization fault, are the main reason for injecting harmonics to the phase current. Six-step operation of the BLDC leads to the specific extrema in the phase currents at each switching instance. These patterns are treated analytically.

Back-EMF is an important signal in the diagnosis of the demagnetization fault, because flux disturbance caused by this fault influences Back-EMF waveforms. It is possible to separate the effect of each individual PM on each coil by knowing individual coils offset angles (Hanselman, 2003; Goktas et al., 2016). Suppose the following Fourier series:

$$e_{ac} = \sum_{n=-\infty}^{+\infty}\left(\sum_{k=1}^{p}(-1)^{k-1}d_k e^{jn(k-1)\frac{360}{p}}\right)e^{jn\theta_{cac}}E_n e^{jn\theta_m} \qquad (2)$$

$$\theta_{cac} = (c-1)\frac{360}{p} \tag{3}$$

describes the induced voltage in $c^{th}$ coil of phase a with separated effects of each individual magnet in a p-pole PM motor where $d_k$ is between 0 and 1 introducing demagnetization fault severity of each magnet, $E_n$ is the amplitude of $n^{th}$ Fourier series coefficients, $\theta_m$ is the mechanical position of the rotor, and $\theta_{cac}$ is the coil angle of $c^{th}$ coil which can be calculated by (3). Taking coil angles for all $N_c$ coils into account, the induced voltage in phase a is as follows:

$$e_a = \sum_{n=-\infty}^{+\infty}\left(\sum_{c=1}^{N_c}(-1)^{c-1}e^{jn\theta_{cac}}\right) \times\left(\sum_{k=1}^{p}(-1)^{k-1}d_k e^{jn(k-1)\frac{360}{p}}\right)E_n e^{jn\theta_m} \tag{4}$$

The first part in (4) corresponds to the distribution of the coils in stator slots for a particular winding layout:

$$S_{wan} = \sum_{c=1}^{N_c}(-1)^{c-1}e^{jn\theta_{cac}} \tag{5}$$

The second part in (4) is related to the number of rotor magnets and fault severity of the magnets:

$$S_{pmn} = \sum_{k=1}^{p}(-1)^{k-1}d_k e^{jn(k-1)\frac{360}{p}} \tag{6}$$

And the last part forms the shape of the Back-EMF waveform for each individual coil. For a balanced winding, induced voltages in other phases can be calculated by shifting the coil angle $\theta_{cac}$ in $S_{wan}$ part by 120°:

$$e_a = \sum_{n=-\infty}^{+\infty}\left(S_{wbn}S_{pmn}E_n e^{jn\theta_m}\right) \tag{7}$$

$$e_c = \sum_{n=-\infty}^{+\infty}\left(S_{wcn}S_{pmn}E_n e^{jn\theta_m}\right) \tag{8}$$

Similarly, line-to-line Back-EMF are expressed by subtracting two corresponding phase Back-EMF for the line Back-EMF of phase a and phase b:

$$e_{ab} = \sum_{n=-\infty}^{+\infty}S_{wbn}\left[1-e^{jn120}\right]S_{pmn}E_n e^{jn\theta_m} \tag{9}$$

Although the fault frequency components in (1) are observed in the phase Back-EMF, Eqn. (9) indicates that some components can be disappeared in the line-to-line Back-EMF due to the lack of phase difference which depends on the winding configuration and number of poles and slots.

Suppose the induced voltages of the coils are perfect trapezoidal waveforms with a flat-top of 120 electrical degrees; as an ideal case for a BLDC motor. Therefore, the following fourier series coefficients:

$$E_n = -\frac{j}{2}\left(\frac{12}{\pi^2}\right)\left(\frac{\sin\frac{n\pi}{6}+\sin\frac{5\pi}{6}}{n^2}\right) \tag{10}$$

Can be directly calculated by its function or by subtraction of two triangular waveforms.

*2.4 Experimental Setup*

The proposed algorithm is verified by simulation of experiments. Simulations are performed at healthy condition and fault conditions. The parameters of the BLDC are summarized in Table I.

BLDC upper PWM-based inverter drive in speed control mode is used to operate the motor for experimental verification. The switching frequency of the inverter is 625 kHz and it has speed and position feedback system using hall sensors. The overall experimental setup is illustrated in Fig. 3.

**Table 1** The parameters of BLDC motor.

| **Parameters** | **Value** | |
|---|---|---|
| Rated Power | 800 | W |
| Rated Voltage | 48 | V |
| Rated Current | 11 | A |
| Rated Speed | 3,000 | rpm |
| Phase | 3 | - |
| Slots of Stator | 18 | - |
| Poles | 16 | - |

The important equipment for testing Demagnetization Fault in BLDC motor is Power Supply, Current Probe, BLDC motor, DC motor and Computer as shown in Fig. 3.

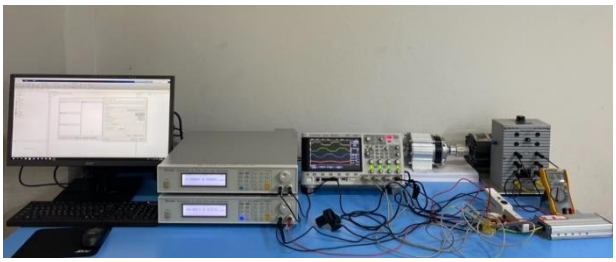

**Figure 3** Overall experimental setup

To detect the motor's stator current and Back-EMF signals, the electrical signal flowing through the motor is measured.


(a) (b) (c) (d)

**Figure 4** Photograph of Demagnetization Faults
(a) Stator (b) 0BB (c) 1BB (d) 2BB

The current data is recorded using an oscilloscope with a sampling of 2 kHz and a total of 10,000 data records, so the frequency resolution is 0.2 Hz. The simulation of fracture condition of the permanent magnet in BLDC Motor is divided into 3 cases: 1. Normal permanent magnet (0BB), 2. Damaged permanent magnet 1 rod (1BB) and 3. Damaged permanent magnet 2 rod (2BB) as follows: Fig. 4. and an example of the motor current and voltage signal is shown in Fig. 5.

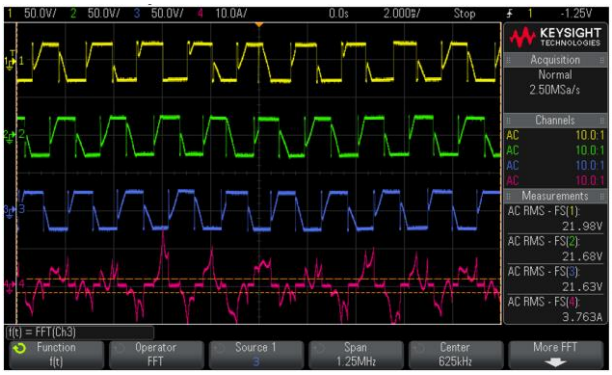


**Figure 5** Signal of current and Back-EMF

*2.5 Experimental Results*

The harmonics effect on the permanent magnet damage is applied as the default value for the input as shown in Figures 6, 7 and table 2. 1. Frequency of third order harmonics in the Back-EMF 2. Magnitude of third order harmonics in the Back-EMF 3. frequency of third order harmonics in the motor current 4. Magnitude of third order harmonics in the motor current.

**Table 2** Data of Harmonic Components.

| Condition | Input | | | | Target |
|---|---|---|---|---|---|
| | X1 | X2 | X3 | X4 | Y1 |
| 0BB | 2.58 | 1245.63 | 0.71 | 2910.00 | 1 |
| 0BB | 3.08 | 1246.88 | 0.76 | 2920.00 | 1 |
| 0BB | 2.96 | 1247.50 | 0.69 | 2920.00 | 1 |
| 0BB | 2.96 | 1248.13 | 0.74 | 2920.00 | 1 |
| 1BB | 2.77 | 1326.88 | 0.95 | 1760.63 | 2 |
| 1BB | 2.99 | 1327.50 | 1.28 | 1763.13 | 2 |
| 1BB | 3.25 | 1328.75 | 0.83 | 1763.75 | 2 |
| 1BB | 2.96 | 1329.38 | 1.09 | 1766.25 | 2 |
| 2BB | 2.17 | 1410.00 | 0.74 | 1523.75 | 3 |
| 2BB | 2.56 | 1410.00 | 0.86 | 1524.38 | 3 |
| 2BB | 2.50 | 1410.00 | 0.88 | 1525.63 | 3 |
| 2BB | 2.66 | 1410.00 | 0.92 | 1525.63 | 3 |

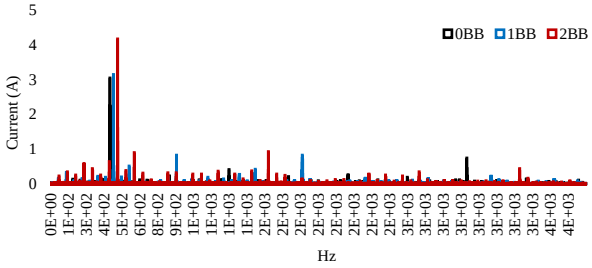


**Figure 6** 3rd Orde of Harmonic Components of Motor Current

The harmonic analysis of stator phase currents under fault conditions has been already illustrated in Fig. 6. The harmonic analysis of rotor Back-EMF under fault conditions has been already illustrated in Fig. 7.

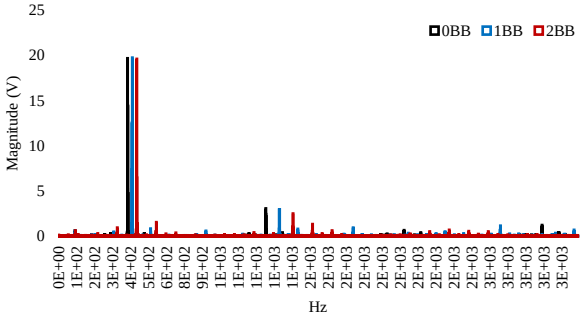


**Figure 7** 3rd Order of Harmonic Components of Back-EMF

## 3. ADAPTIVE NEURO-FUZZY INFERENCE SYSTEM (YILMAZ & AYAZ, 2009)

ANFIS is an implementation of a fuzzy logic inference system with the architecture of a five-layer feed-forward network. With this way ANFIS uses the advantages of learning capability of neural networks and inference mechanism similar to human brain provided by fuzzy logic. The architecture of ANFIS with two inputs, one output and two rules are given in Fig. 8. Here *x*, *y* are inputs, *f* is output, the circles represent fixed node functions and squares represent adaptive node functions. This is a Sugeno type

Fuzzy system, where the fuzzy *IF-THEN* rules have the following form:

Rule$_1$:

IF $x$ is $A_1$ and $y$ is $B_1$ THEN $f_1 = p_1x + p_1x + q_1y + r_1$

Rule$_2$:

IF $x$ is $A_2$ and $y$ is $B_2$ THEN $f_2 = p_2x + p_2x + q_2y + r_2$

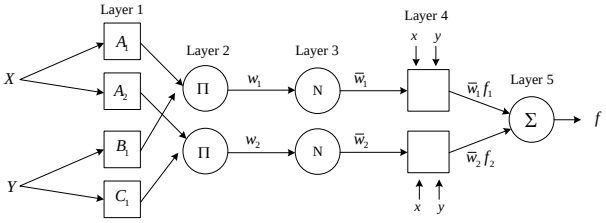


**Figure 8** ANFIS architecture.

The operation of each layer is as follows: Here the output node *i* in layer *l* is denoted as $O_i^l$ .

Layer 1 is fuzzification layer. Every node *i* in this layer is an adaptive node with node function

$$O_i^l = \mu_{A_i}(x), \quad O_{i+2}^l = \mu_{A_i}(x), \quad i = 1,2 \tag{11}$$

Where *x* is the input to $i^{th}$ node, $O_i^1$ is the membership grade of *x* in the fuzzy set $A_i$ . Generalized bell membership function is popular method for specifying fuzzy sets because of their smoothness and concise notation, and defined as

$$\mu_{A_i}(x) = \frac{1}{1+\left[\left(\frac{x-c_i}{a_i}\right)^2\right]^{b_i}} \tag{12}$$

Here $\{a_i, b_i, c_i\}$ is the parameter set of the membership function. The center and width of the membership function is varied by adjusting $c_i$ and $a_i$ .The parameter $b_i$ is used to control the slopes at the crossover points. Fig. 9 shows the physical meaning of each parameter in a generalized bell function. The parameters in this layer are called premise parameters. This layer forms the antecedents of the fuzzy rules (*IF* part).

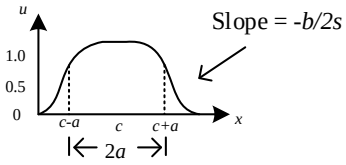


**Figure 9** Generalized bell function.

Layer 2 is rules layer. Every node in this layer is a fixed node and contains one fuzzy rule. The output is the product of all incoming signals and represents the firing strength of each rule.

$$O_i^2 = w_1 = \mu_{A_i}(x)\mu_{B_i}(y) \tag{13}$$

Layer 3 is normalization layer. Every node in this layer is a fixed node and $i^{th}$ node calculates the ratio of $i^{th}$ rule's firing strength to the sum of all rules' firing strengths. Outputs of this layer are called normalized firing strengths computed as

$$O_i^3 = \overline{w_i} = \frac{w_i}{w_1 + w_2}, i = 1,2 \tag{14}$$

Layer 4 is consequent layer. Every node in this layer is an adaptive node and computes the values of rule consequent (*THEN* part) as

$$O_i^4 = \overline{w_i} f_1 = \overline{w_i}(p_i x + q_i y + r_i) \tag{15}$$

Here *i w* is the output of Layer 3 and the parameters $\{p_i, q_i, r_i\}$ are called as consequent parameters.

Layer 5 is summation layer and consists of single fixed node which calculates the overall output as the summation of all incoming signals as

$$O_i^5 = \sum_i \overline{w_i} f_i = \frac{\sum_i w_i f_i}{\sum_i w_i} \tag{16}$$

Learning of ANFIS is done using hybrid learning procedure which combines back-propagation gradient descent and least squares method for identification of premise and consequent parameters.

An ANFIS model-based fault detector for a BLDC motor has been designed and tested using simulations. The results indicated that, regardless of the loading condition, the proposed scheme is capable of detecting Demagnetization. The next step is to test whether the proposed fault detection methodology is able to detect the existence of Demagnetization in a practical BLDC motor.

**Table 3** Parameter for training in ANFIS.

| | **Parameter** | |
|---|---|---|
| **Input** | Frequency of Third order harmonics in the Back-EMF | X1 |
| | Magnitude of Third order harmonics in the Back-EMF | X2 |
| | Frequency of Third order harmonics in the Motor Current | X3 |
| | Magnitude of Third order harmonics in the Motor Current | X4 |
| **Output** | Demagnetization (Healthy (0BB), Unhealthy (1BB, 2BB)) | Y1 |

An ANFIS method detects permanent magnet damage in this study. Use the analysis of ANFIS that has a mixed structure of the fuzzy logic system and artificial neural networks methods. In the FLS part, choose membership function as triangular and choose the principle of function. Approximation is surgeon fuzzy model and in ANN part choose feed-forward network, there is transfer function at hidden layer and output layer is tan-sigmoid transfer function (tensing) and linear transfer function (purlin) respectively and have a learning style back-propagation learning. The structure of ANFIS is shown in Fig.10., which consists of 4 input layers (X1, X2, X3, X4**)** and 1 output layer Y1 **(**0BB, 1BB, 2BB) as in Table 3.

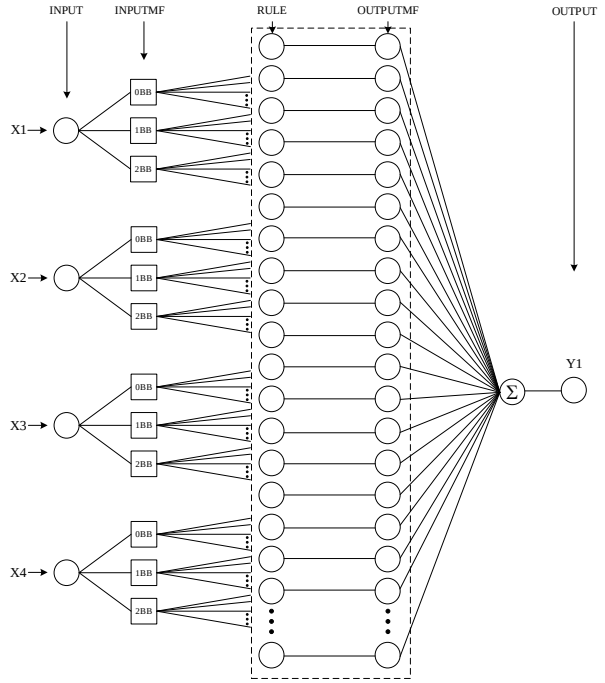


**Figure 10** The structure of ANFIS

The structure of ANFIS in this research. The learning results of the program can be displayed with a surface chart between the input and output relationships as shown in Fig. 11.

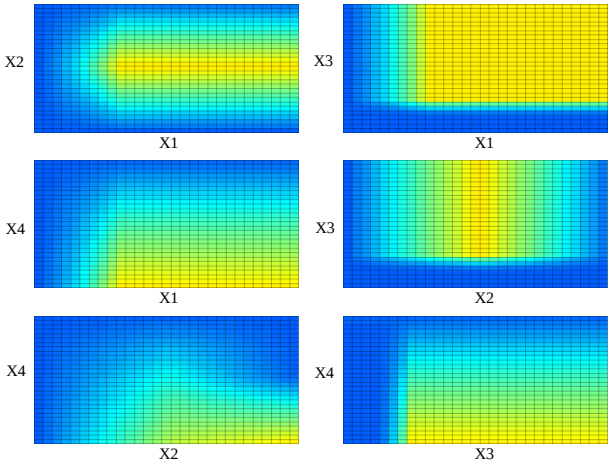


**Figure 11** Surface

The results of the permanent magnet abnormality test with ANFIS can be shown and compared with the results of the detection of abnormalities occurring in the BLDC motor as shown in Fig. 12. From the figure, it shows that the detected result with the value. Targets are of the same value. It has an ANFIS learning error of 3.62E-03 and an accuracy in detecting an anomaly of 98.81%.

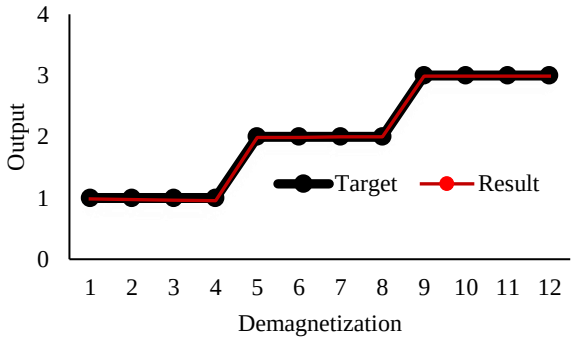


**Figure 12** Result of ANFIS

## 4. CONCLUSION

In this paper, the demagnetization fault detection of brushless DC electric motor using adaptive neuro-fuzzy inference system (ANFIS). The ANFIS method has been utilized to obtain data collection of the harmonic components of Back-EMF and harmonic components of current. Comparison in terms of accuracy and MSE for ANFIS is demonstrated. The results obtained show that the best MLP training algorithm has the best accuracy (98.81%) and MSE (3.62E-03) compared with others training algorithms. The test results are reliable and can be applied for the future.

## 5. ACKNOWLEDGMENT

The authors would like to thanks University of Phayao particular that such as Faculty of Engineering for supporting the finance for research, material and equipment, advising staffs in this project.

## 6. REFERENCES

Albrecht, P. F., Appiarius, J. C., McCoy, R. M., Owen, E. L., & Sharma, D. K. (1986). Assessment of the reliability of motors in utility applications-Updated. IEEE Transactions on Energy conversion, (1), 39-46.

Kim, H. K., Kang, D. H., & Hur, J. (2015). Fault detection of irreversible demagnetization based on space harmonics according to equivalent magnetizing distribution. IEEE Transactions on Magnetics, 51(11), 1-4.

Kang, D. H., Kim, H. K., & Hur, J. (2015, September). Irreversible demagnetization diagnosis of IPM-type BLDC motor using BEMF harmonic characteristics based on space harmonics. In 2015 IEEE Energy Conversion Congress and Exposition (ECCE) (pp. 6956-6961). IEEE.

Li, Z. X., Yang, G. L., Fan, Y. M., & Li, J. H. (2021). Irreversible demagnetization mechanism of permanent magnets during electromagnetic buffering. Defence Technology, 17(3), 763-774.

Usman, A., & Rajpurohit, B. S. (2020). Modeling and Classification of Stator Inter-Turn Fault and Demagnetization Effects in BLDC Motor Using Rotor Back-EMF and Radial Magnetic Flux Analysis. IEEE Access, 8, 118030-118049.

Usman, A., Sharma, V. K., & Rajpurohit, B. S. Harmonic Analysis of a BLDC Motor Under Demagnetization Fault Conditions. In 2020 IEEE 9th Power India International Conference (PIICON) (pp. 1-5). IEEE.

Usman, A., Joshi, B. M., & Rajpurohit, B. S. (2019, October). Modeling and analysis of demagnetization faults in BLDC motor using hybrid analytical-numerical approach. In IECON 2019-45th Annual Conference of the IEEE Industrial Electronics Society (Vol. 1, pp. 1198-1203). IEEE.

Kim, H. K., & Hur, J. (2016). Dynamic characteristic analysis of irreversible demagnetization in SPM-and IPM-type BLDC motors. IEEE Transactions on Industry Applications, 53(2), 982-990.

Kim, B. C., Lee, J. H., & Kang, D. W. (2020). A study on the effect of eddy current loss and demagnetization characteristics of magnet division. IEEE Transactions on Applied Superconductivity, 30(4), 1-5.

Kim, H. K., Hur, J., Kim, B. W., & Kang, G. H. (2010, September). Characteristic analysis of IPM type BLDC motor considering the demagnetization of PM by stator turn fault. In 2010 IEEE Energy Conversion Congress and Exposition (pp. 3063-3070). IEEE.

Usman, A., & Rajpurohit, B. S. (2020, January). Numerical Analysis of Stator Inter-turn Fault and Demagnetization effect on a BLDC Motor using Electromagnetic Signatures. In 2020 IEEE International Conference on Power Electronics, Smart Grid and Renewable Energy (PESGRE2020) (pp. 1-6). IEEE.

Madhav, N., & Sadakale, R. (2020, July). Analysis of demagnetized BLDC Motor using MATLAB Simulink model and AWT analysis. In 2020 11th International Conference on Computing, Communication and Networking Technologies (ICCCNT) (pp. 1-5). IEEE.

Kim, D. H., Im, J. H., Zia, U., & Hur, J. (2020, October). Online Detection of Irreversible Demagnetization Fault with Non-excited Phase Voltage in Brushless DC Motor Drive System. In 2020 IEEE Energy Conversion Congress and Exposition (ECCE) (pp. 748-753). IEEE.

Mati, D., & Kuli, F. (2010, September). Artificial neural networks broken rotor bars induction motor fault detection. IEEE. In Symposium on Neural Network Applications in Electrical Engineering (pp. 23-25).

Drira, A., & Derbel, N. (2011, March). Classification of rotor fault in induction machine using Artificial Neural Networks. In Eighth International Multi-Conference on Systems, Signals & Devices (pp. 1-6). IEEE.

Kolla, S. R., & Altman, S. D. (2007). Artificial neural network based fault identification scheme implementation for a three-phase induction motor. ISA transactions, 46(2), 261-266.

Dias, C. G., & Chabu, L. E. (2008, June). A fuzzy logic approach for the detection of broken rotor bars in squirrel cage induction motors. In 2008 IEEE International Conference on Fuzzy Systems (IEEE World Congress on Computational Intelligence) (pp. 1987-1991). IEEE.

Zouzou, S. E., Laala, W., Guedidi, S., & Sahraoui, M. (2009, December). A fuzzy logic approach for the diagnosis of rotor faults in squirrel cage induction motors. In 2009 Second International Conference on Computer and Electrical Engineering (Vol. 2, pp. 173-177). IEEE.

Laala, W., Guedini, S., & Zouzou, S. (2011, September). Novel approach for diagnosis and detection of broken bar in induction motor at low slip using fuzzy logic. In 8th IEEE Symposium on Diagnostics for Electrical Machines, Power Electronics & Drives (pp. 511-516). IEEE.

Souad, L., Youcef, M., & Samir, M. (2017, October). Use of Neuro-fuzzy technique in diagnosis of rotor faults of cage induction motor. In 2017 5th International Conference on Electrical Engineering-Boumerdes (ICEE-B) (pp. 1-4). IEEE.

Moghadasian, M., Shakouhi, S. M., & Moosavi, S. S. (2017, September). Induction motor fault diagnosis using ANFIS based on vibration signal spectrum analysis. In 2017 3rd International Conference on Frontiers of Signal Processing (ICFSP) (pp. 105-108). IEEE.

Ballal, M. S., Khan, Z. J., Suryawanshi, H. M., & Sonolikar, R. L. (2007). Adaptive neural fuzzy inference system for the detection of inter-turn insulation and bearing wear faults in induction motor. IEEE Transactions on Industrial Electronics, 54(1), 250-258.

Faiz, J., & Mazaheri-Tehrani, E. (2017). A novel demagnetization fault detection of brushless DC motors based on current time-series features. In 2017 IEEE 11th International Symposium on Diagnostics for Electrical Machines, Power Electronics and Drives (SDEMPED) (pp. 160-166). IEEE.

Yilmaz, M. S., & Ayaz, E. (2009, May). Adaptive neuro-fuzzy inference system for bearing fault detection in induction motors using temperature, current, vibration data. In IEEE EUROCON 2009 (pp. 1140-1145). IEEE.

Hanselman, D. C. (2003). Brushless permanent magnet motor design. The Writers' Collective.

Goktas, T., Zafarani, M., & Akin, B. (2016). Discernment of broken magnet and static eccentricity faults in permanent magnet synchronous motors. IEEE Transactions on Energy Conversion, 31(2), 578-587.

### 7. BIOGRAPHIES (OPTIONAL)

Kreangsuk Kraikitrat
Graduation B.Eng. (Electrical Engineering), and M.Eng. (Electrical Engineering), and Ph.D. (Electrical Engineering) respectively at Naresuan University. Currently working as a professor at the Department of Electrical Engineering Faculty of Engineering, University of Phayao.

Bunyarit Wangngon
Graduation B.Eng. (Electrical Engineering), and M.Eng. (Electrical Engineering), and Ph.D. (Electrical Engineering) respectively at Naresuan University. Currently working as a professor at the Department of Electrical Engineering Faculty of Technology Lanna Phitsanulok.